Molecular Properties Investigation of a Substituted Aromatic Mannich Base: Dynamic and Static Models†

Aneta Jezierska,* Jarosław J. Panek, and Aleksander Filarowski

University of Wrocław, Faculty of Chemistry, 14 F. Joliot-Curie, 50-383 Wrocław, Poland

Received November 3, 2006

An analysis of the hydrogen bridge of a Mannich base-type compound [3,5,6-trimethyl-2(*N*,*N*-dimethylaminomethyl)phenol, TMM] was performed according to the Car−Parrinello molecular dynamics (CPMD) scheme. A classical treatment of nuclei coupled with a first-principle potential energy surface was obtained from molecular dynamics simulation. Dipole moment values were collected during CPMD trajectory acquisition and subsequently used for the data analysis. The vibrational features and the intramolecular hydrogen-bond properties in the gas phase and solid state of the TMM compound were analyzed on the basis of widely used approaches: Fourier transformation of the autocorrelation function of both the atomic velocities and dipole moments. In addition, the time evolution of the structural parameters related to the hydrogen bond was carried out. The optimally localized Wannier functions served to describe the electronic structure of the Mannich base studied. The second part of the TMM compound study was performed in vacuo on the basis of density functional theory and second-order Møller−Plesset perturbation theory. The potential energy functions were used to solve the 1-D vibrational Schroedinger equation for the proton motion. This enabled a prediction of the anharmonic vibrational levels of the intramolecular hydrogen bond. The description of the electron density topology of the TMM molecule was carried out using the atoms in molecules theoretical framework. The computational results were further compared with the infrared spectra in the solid state.

I. INTRODUCTION

Molecular modeling techniques are widely used nowadays in various branches of science and industry. The enormous progress in computer hardware design enables the simulation of huge biologically relevant systems. Recently, the first molecular dynamics (MD) simulation of a living organism (complete satellite tobacco mosaic virus) was reported.[1] At the same time, the rapid development of new methodologies and software allows us to use increasingly more accurate methods to investigate chemical, physical, and even biological properties.[2,3] Not so long ago, there was a large gap between the world of "static" quantum chemical calculations and the real experimental domain of macroscopic systems. This gap has been successfully bridged by molecular dynamics methods, which combine a microscale description of atoms with macroscopic statistical thermodynamics.[4−6] Currently, two frontier fields of contemporary computational chemistry are distinguished: drug design (or, more generally, biochemical investigations) and material science (e.g., nanotechnology, molecular devices, and the support of single-molecule experiments). Diverse techniques of computational chemistry are widely used in drug design. Quantitative structure−activity/−property relationship methods provide theoretical models for further molecular activity/property predictions.[7−11] Drug/receptor binding investigations based on docking methods[12−16] give insight into interactions at the molecular level. Computer simulations of proteins, nucleic acids, or other biologically relevant systems[17−19] are able to shed light on significant and important processes, the understanding of which is crucial for further drug development and improvement of human life quality. The computationally obtained models and molecular property predictions are also very useful in material science. The models are able to explain and predict some molecular properties significant in new materials design,[20−22] which is crucial for further industrial applications. An example of such a property is the molecular conductivity, or rather voltage−current response curve, used in the design of molecular switches and logical gates.[23−25]

The hydrogen bond, although much weaker than typical chemical covalent interactions, has special influence on the molecular and macroscopic properties of compounds.[26,27] The intramolecular hydrogen bond is responsible for structure stabilization, while the intermolecular hydrogen bond is involved in intermolecular interactions evident as, for example, crystal packing forces or DNA strand stability factors. Both types of hydrogen bond are relevant in various branches of contemporary science. Here, a computational study of molecular properties, that is, the intramolecular hydrogen bond, vibrational properties, and electronic structure, was performed on the basis of the Car−Parrinello molecular dynamics (CPMD) method.[28] The CPMD approach has been applied successfully to the computational treatment of the hydrogen bond.[29−33] The greatest advantage of the dynamical models is access to a description of the time evolution of the system, which gives rise to the possibility of studying condensed-phase parameters (distribution functions and diffusion constants). The CPMD method

† Dedicated to Professor Nenad Trinajstić on the occasion of his 70th birthday.

* Corresponding author phone: +48 71 3757 308; fax: +48 71 3282 348; anetka@elrond.chem.uni.wroc.pl.

10.1021/ci600490s CCC: $37.00
Published on Web 04/04/2007

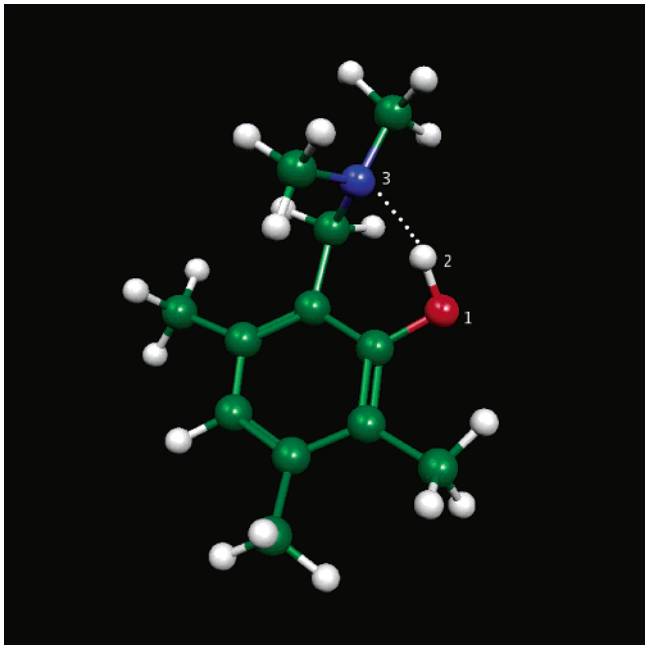

Figure 1. Structure of the Mannich base, 3,5,6-trimethyl-2(*N*,*N*-dimethylaminomethyl)phenol (TMM) with color coding (carbon, green; hydrogen, white; nitrogen, blue; oxygen, red). The structure was investigated during the gas-phase MD simulations. Only atoms involved in the hydrogen bond are labeled.

is an electronic structure approach with the evaluation of the electron density being performed on the fly. This in turn makes possible calculations of the evolution of the dipole moment, infrared spectra,[34,35] and excited states.[36,37] Methods of including quantum corrections to the nuclear dynamics have also been developed.[38] In addition, special methodologies for biologically relevant large systems have recently been implemented.[39−41] Their common idea is a two-level description of a system involving a quantum-mechanically investigated core and an outer layer regarded at the molecular mechanics level. Fully classical molecular dynamics simulations are also useful in hydrogen-bonding studies, for example, with respect to solvent structuring around a solute[42] or in biomolecular studies.[43,44] However, most hydrogen-bonding studies rely on a static description of the system using advanced electronic structure methods such as the density functional theory[45] (DFT) or correlated ab initio approaches, for example, Møller−Plesset multibody perturbation theory.[46]

The main goal of this study was an investigation of the intramolecular hydrogen bond and vibrational properties based on molecular dynamics and static models obtained via DFT and second-order Møller−Plesset (MP2) calculus. The system chosen for this study, 3,5,6-trimethyl-2(*N*,*N*-dimethylaminomethyl)phenol (TMM), belongs to the Mannich base family. Mannich base type compounds have been found interesting due to their biological activity. The cytotoxic properties of some Mannich bases[47] can be refined to provide antibacterial, antifungal, and antiviral activity in the norfloxacin[48] and isatin families,[49−54] or related compounds.[55−57] Mannich bases have also found industrial application in polymer chemistry.[58]

Members of a particular class of the Mannich base family, namely, ortho Mannich bases, are good models for intramolecular hydrogen-bond studies. Their six-membered pseudo-ring closed by a hydrogen bond is usually nonplanar.[59] The presence of a saturated C−C bond in the ring reduces electronic coupling between the donor and acceptor atoms. Hydrogen-bridge properties of Mannich bases are easily modified by substitution in the aromatic ring. A good example, considered further in this study, is TMM. The crystal structure and spectroscopic properties of TMM have already been reported.[60] The anomalous strengthening of the intramolecular hydrogen bond in TMM with respect to similar Mannich bases has been attributed to the steric repulsive interactions between the donor oxygen atom and the neighboring methyl group.

The outline of the article is a follows: details of collecting the solid-state infrared spectrum (IR) experimental data and the computational methodology are described in section II; results obtained on the basis of the experimental and

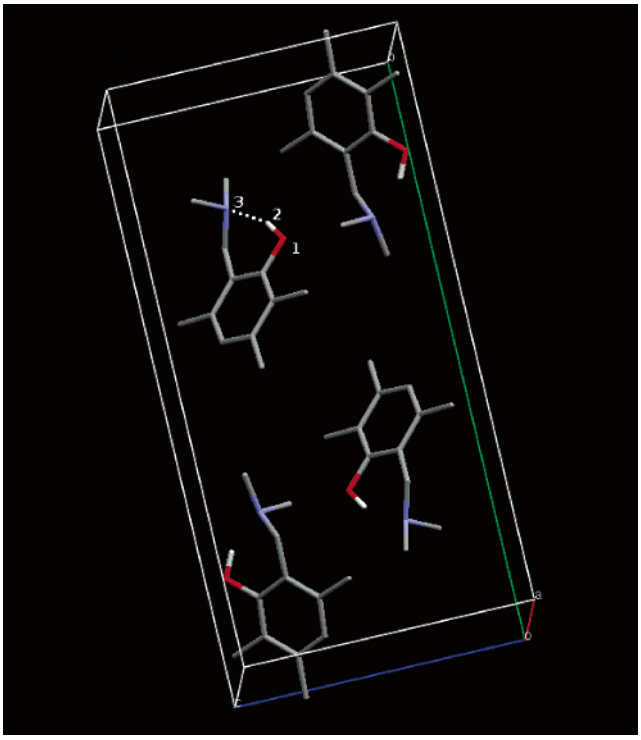

Figure 2. Theoretical model of the Mannich base studied [3,5,6-trimethyl-2(*N*,*N*-dimethylaminomethyl)phenol (TMM)] used for solid-state calculations (taken directly from the experimental crystal data). Atoms involved in the hydrogen bond are marked. Color coding: gray, carbon; blue, nitrogen; red, oxygen; white, bridge proton.

Table 1. Comparison of the Experimental and Calculated Spectroscopic Data of the OH Stretching Mode (in cm^{-1}) of the TMM Compound

	gas phase	solid state
experimental	2200−3400[a] cm^{-1}	ca. 1700[b]−3100 cm^{-1}
CPMD results, atomic velocity power spectra	2350−3250 cm^{-1}	1900−3000 cm^{-1}
CPMD results, dipole moment analysis	2200−3250 cm^{-1}	1800∼2900[c] cm^{-1}
static DFT approach	2715.7 cm^{-1}	
static MP2 approach	2777.3 cm^{-1}	

[a] The experiment in CCl_4 solution, ref 60. [b] Possibly overlapped by the ring modes. [c] Overlap with the CH modes prevented us from obtaining a more precise reading.

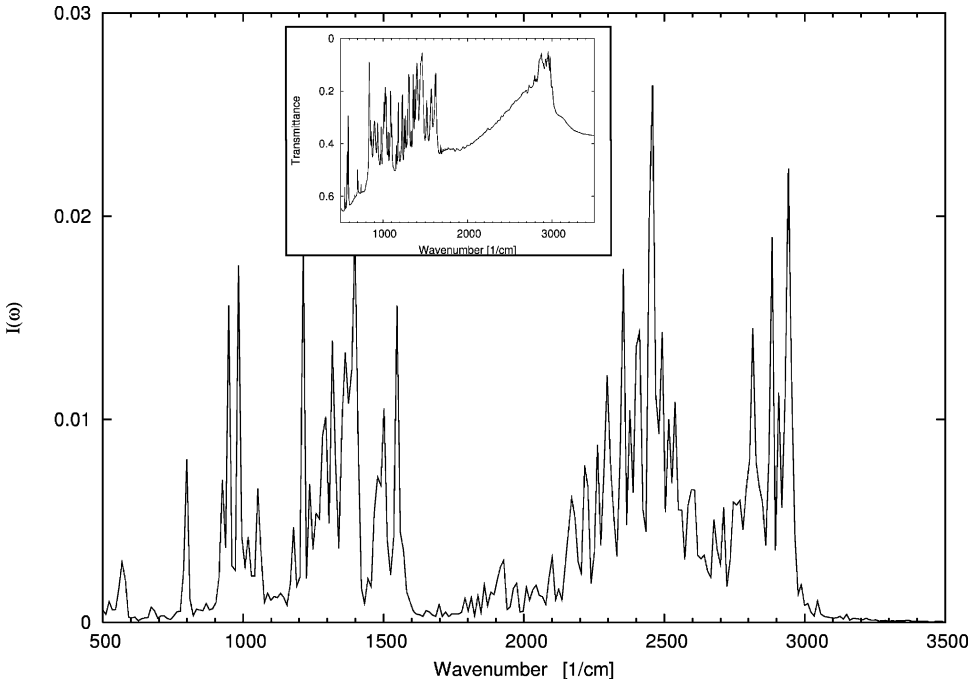

Figure 3. Predicted IR spectrum of the TMM model in the solid state. The experimental solid-state spectrum is presented in the inset.

computational studies are discussed in section III, and the final conclusions are given in section IV.

II. EXPERIMENTAL AND COMPUTATIONAL PROCEDURES

Solid-State Infrared Spectrum Measurement. The synthesis, crystal structure, and infrared characterization in CCl_4 solution were published previously.[60] The IR spectrum of solid-state TMM was recorded on a Bruker IFS-66/S FT-IR spectrophotometer with 2 cm^{-1} resolution. A sample of TMM was melted between KRS-5 thallium bromide−iodide plates, and the spectrum was recorded after the sample cooled down. Additional data collection after 1 h yielded the same spectrum as the first measurement.

CPMD Simulation. Molecular dynamics simulation was performed on the basis of the methodology of Car and Parrinello[28] using the CPMD v.3.9.2 program.[61] Initial structure optimization for the gas-phase and solid-state calculations was carried out with the Schlegel Hessian.[62] Calculations were performed on the basis of DFT,[45] with the approximation for exchange and correlation energy proposed by Perdew et al.[63] The pseudopotentials proposed by Troullier and Martins[64] were used to replace the core electrons of the atoms in the system studied. A kinetic energy cutoff of 70 Ry was applied for the plane-wave basis set during the simulation. The time step was consistently set to 3 au. A fictitious electron mass parameter (EMASS) equal to 400 au was applied to reproduce the orbital dynamics. MD simulations were performed at a temperature of 300 K with allowed variations of ±50 K. The initial period of molecular dynamics (ca. 10 000 steps) was taken as the equilibration phase and was not further analyzed. The power spectra of atomic velocities for the gas-phase and solid-state models were generated respectively. In addition, the dipole moment values were collected during the MD run and were further used for generating the IR spectrum. A program for autocorrelation function calculations was applied for this purpose. The time evolution of the interatomic distances related to the intramolecular hydrogen bond was analyzed using programs developed in our laboratory. As a last step of our molecular dynamics computational study, optimally localized Wannier functions were calculated.[65,66] Additional technical details applied in the gas-phase and solid-state calculations are listed below.

CPMD Calculations in Vacuo. Molecular dynamics in the gas phase were performed in a cubic cell of $a = 13.5$ Å. The data collection time was ca. 5.6 ps. The Mannich base studied contains 33 atoms, and its chemical structure is presented in Figure 1.

CPMD Solid-State Calculations. Solid-state molecular dynamics were performed on the basis of available experimental data.[60] The experimental monoclinic unit cell with $a = 5.440$ Å, $b = 20.818$ Å, $c = 10.139$ Å, and $\beta = 95.92°$ was used to build a model for further computational study. The Cambridge Structural Database crystal code for the compound studied is LEQWIN. The unit cell (see Figure 2) contains four TMM molecules, 132 atoms, which makes the model relatively large for an ab initio MD study. The periodic boundary conditions were applied in electrostatic summations with eight neighbors (TESR = 8) in each direction. In view of the size of the simulated crystal cell and lack of intermolecular short contacts in the experimental X-ray structure,[60] the Γ-point approximation was applied for the solid-state study. The data collection time was ca. 11.5 ps.

Static in Vacuo Study. The second part of our TMM study consisted of a detailed investigation of the vibrational and electronic properties of the intramolecular hydrogen bond using various levels of theory: DFT[45] and MP2 perturbation theory.[46] Separate descriptions for each level of theory are below.

Static DFT Study. The geometry optimization of the TMM molecule was carried out using the correlation-consistent cc-pVDZ and cc-pVTZ basis sets.[67,68] The hybrid functional of Becke[69] with the gradient corrections of Lee,

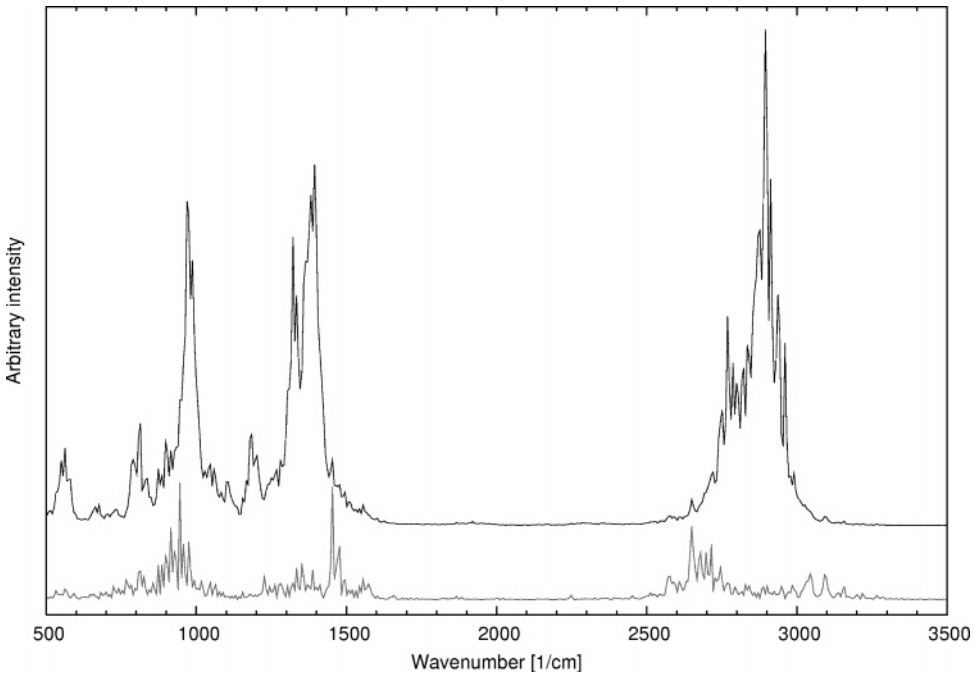

Figure 4. Atomic velocity power spectra obtained for all the atoms (black line) and the H2 hydrogen bridge proton (gray line) of the TMM molecule. Results from the CPMD simulation in vacuo.

Yang, and Parr[70] (B3LYP) was applied as implemented in the Gaussian 03 package,[71] which was used throughout the static study. The obtained molecular structures were confirmed to be minima via harmonic frequency calculations. The potential functions for the proton motion in a hydrogen bridge were constructed by consecutive placing of the hydrogen atom in 40 equidistant positions spanning the circular arc uniquely defined by the optimized coordinates of the donor, proton, and acceptor atoms.[72] At each assumed proton position, the energy of the system and the wavefunction were calculated. The set of the energy values constituting the proton potential profile served in solving the one-dimensional vibrational Schroedinger equation.[73] Since the positions of the remaining nuclei are held constant, this approach cannot retrieve couplings of the investigated O−H mode with other molecular oscillators. These couplings are explicitly taken into consideration by the CPMD simulation. The purpose of both the DFT and MP2 static models is then the study of anharmonic effects in an equilibrium structure of the molecule. Additionally, the importance of the proton quantization can be assessed this way. The use of the static approach enriches the vibrational description of the O−H stretching mode by the effects of both anharmonicity and nuclear quantum corrections for the proton. The generated wavefunctions were further used to calculate the electron density and its derivatives for each proton position on the circular path between the heavy atoms (O···N) involved in the intramolecular hydrogen bond. The theory of atoms in molecules (AIM) proposed by Bader[74] was applied to study this phenomenon. The second application of the AIM theory was the electron density topological study. The electron density properties were estimated at the relevant topological points and compared with some of the criteria proposed by Popelier and Koch.[75] This part of the data analysis was carried out using the original AIMPAC suite of programs.[76]

Static MP2 Study. A very similar, but restricted, analysis was performed using MP2 perturbation theory.[46] The geometry optimization for this electron correlation scheme was carried out with the cc-pVDZ basis set. The potential energy function for the proton motion was tabulated according to the procedure described above. The anharmonic and quantum nuclear corrections are also included in this part of the study, but an electron density analysis was not performed.

The graphic representations presented here were prepared using the Molekel[77] and Mercury[78] visualization programs.

III. RESULTS AND DISCUSSION

Spectroscopic Data Analysis. Table 1 shows both the experimental and calculated vibrational data of interest. Additionally, the relevant part of the solid-state spectrum is shown as an inset in Figure 3. The OH stretching band, located between 1700 and 3100 cm^{-1}, is very broad and overlaps with the CH modes in the upper wavenumber range. The assignment of the lower bound of this spectral feature is also difficult because of the possible overlap with heavy-atom stretching modes. An estimated barycenter of the OH stretching mode is at 2750 cm^{-1}. Other modes related to the bridging proton might be responsible at least partially for the background absorption underlying the lower-frequency bands (800−1700 cm^{-1}). The difference between the solid-state spectrum of the TMM presented here and the previous CCl_4 solution measurements[60] indicates a large increase in proton flexibility and significant hydrogen-bond strengthening in the investigated crystal. It is worth noting that Mannich bases can exist in the solid state either in molecular form or as zwitterions.[59] In the last case, however, intermolecular hydrogen bonds are formed, forcing the molecules to align in cyclic dimers or linear chains. This is not the case for the TMM in the solid state,[60] and the X-ray diffraction data confirm that the IR spectrum presented here is a manifestation of an intramolecular hydrogen bond.

Computational Results. The molecular structure of the analyzed Mannich base type compound—TMM—is presented

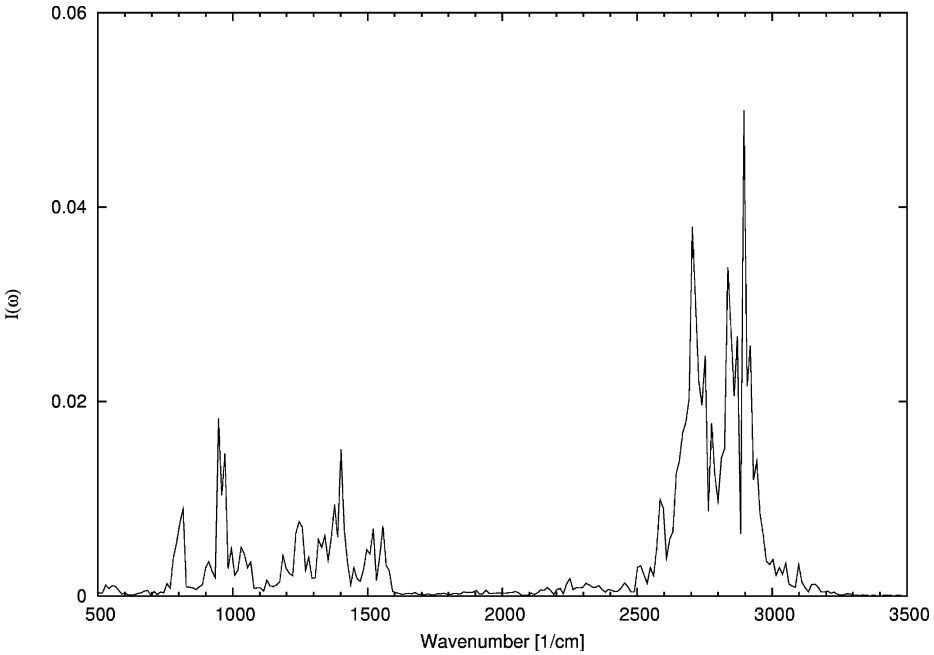

Figure 5. Predicted IR spectrum of the TMM model in the gas phase.

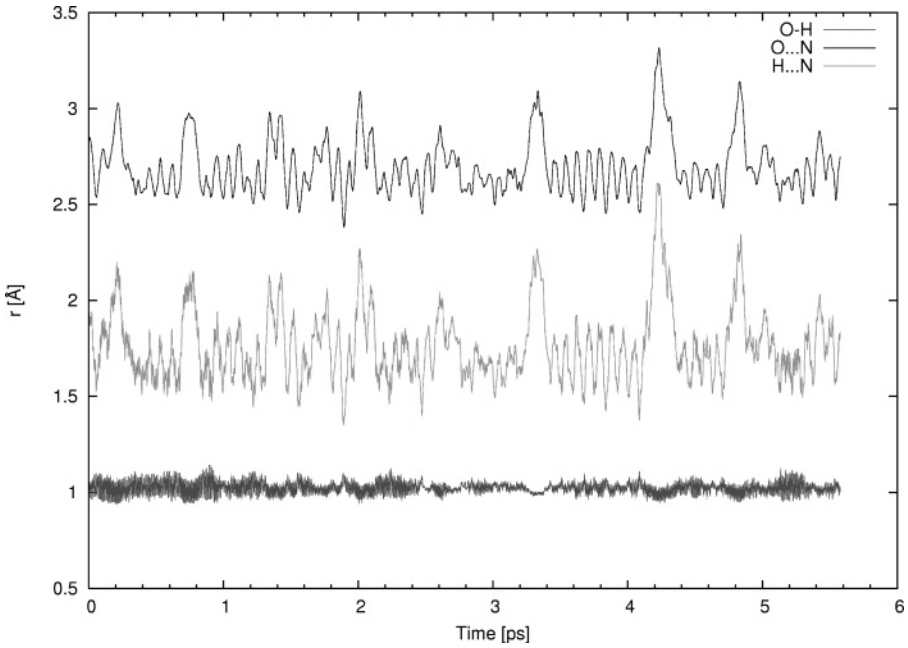

Figure 6. Time evolution of the interatomic distances in the hydrogen bridge of the studied TMM molecule. The data were obtained from MD simulations in vacuo.

Table 2. Comparison of the Experimental and Calculated O···N Distances in the Hydrogen Bridge of the TMM Compound

	gas phase	solid state
experimental		2.628 Å[a]
CPMD results, averages from the MD run	2.684 Å	2.600 Å

[a] X-ray data from ref 60

in Figure 1. In order to reproduce the molecular properties of TMM, several approaches were used, that is, —CPMD, DFT, and MP2 perturbation calculus. In the following paragraphs, the dynamic CPMD models will be presented and discussed for both in vacuo and crystal calculations, followed by the static description of the TMM system.

Car−Parrinello Molecular Dynamics Results. Using the CPMD approach, the time evolution of the molecular properties was investigated on the basis of atomic velocities and the dipole moment collected along the simulated gas-phase trajectory. The dynamic model of the system was constructed to reproduce the spectroscopic data characteristics of the TMM molecule. Two approaches were applied for this purpose. The well-established approach is taking the power spectrum of the atomic velocities.[79] The particular advantage of this method is the possibility to study particular motions (modes) by projecting atomic velocities onto specific vectors, planes, and so forth. On the other hand, the second approach, Fourier transformation of the dipole moment autocorrelation function, enabled us to predict both the

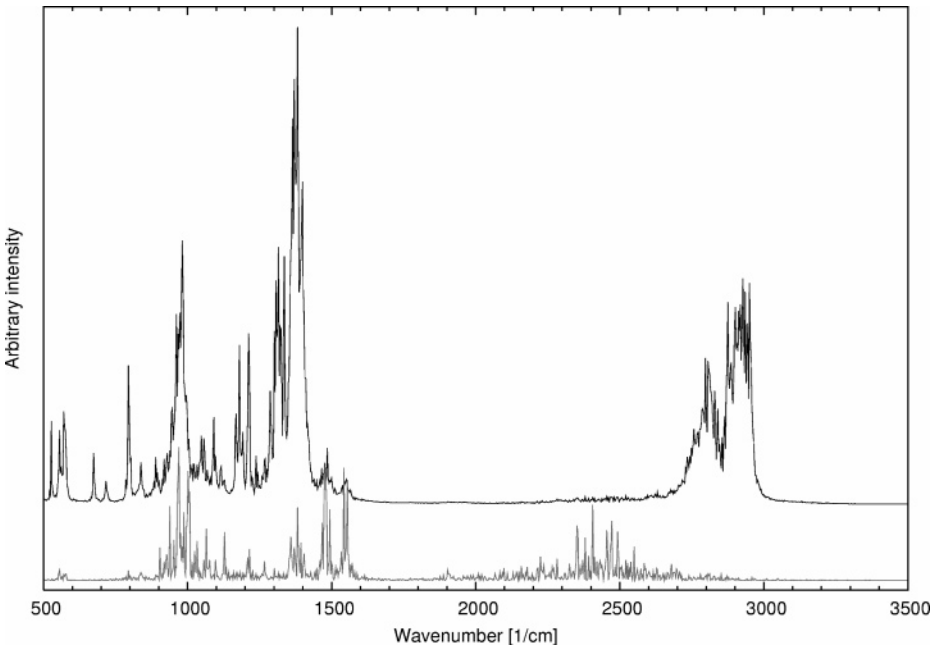

Figure 7. Atomic velocity power spectra obtained for all the atoms (black line) and the H2 hydrogen bridge proton (gray line) of the selected TMM molecule. Results from the CPMD simulation in the solid state.

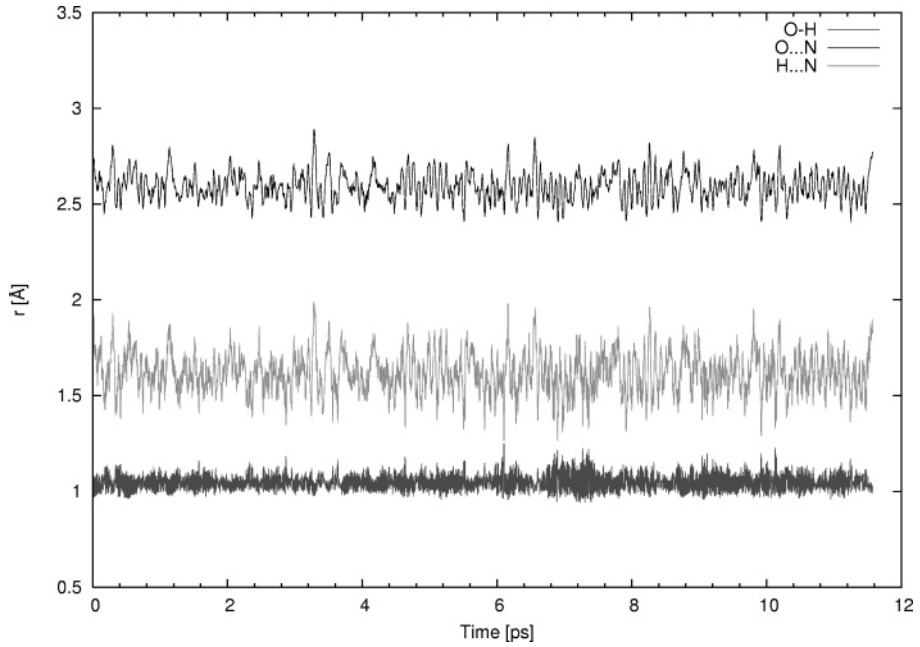

Figure 8. Time evolution of the interatomic distances in the hydrogen bridge of the studied TMM compound. The results presented are for the selected molecule from the solid-state MD simulations.

positions and the intensities of the modes. The use of both approaches will prove especially beneficial in the comparison of the gas-phase and solid-state molecular properties.

A summary of the experimental and calculated IR frequencies is presented in Table 1. The atomic velocity power spectrum from the in vacuo simulation is presented in Figure 4. Special attention was paid to the description of the intramolecular hydrogen bond. The studied TMM compound was found experimentally to have a stronger hydrogen bond than a related Mannich base, 4,5-dimethyl-2(*N*,*N*-dimethylaminomethyl)phenol,[60] as a result of the steric interaction of the ortho methyl group. The steric strain is responsible for the squeezing and shortening the O···N distance. This fact is contrary to the estimates based on pK_a−hydrogen-bond strength correlation rules. The power spectra in Figure 4 show both total and bridge hydrogen atom contributions. The bridge proton power spectrum exhibits signals in three regions: 850−1000 cm^{-1}, 1200−1600 cm^{-1}, and 2350−3250 cm^{-1}. The latter corresponds to the OH stretching, and most of the power density is located from 2650 to 2750 cm^{-1}. The bridge proton contribution is barely visible in the total atomic velocity power spectrum, partially due to overlap with other modes (such as CH stretching frequencies). On the other hand, the Fourier transform of the dipole moment autocorrelation function, shown in Figure 5, is dominated by the bridge proton (2200−3250 cm^{-1}). This is consistent

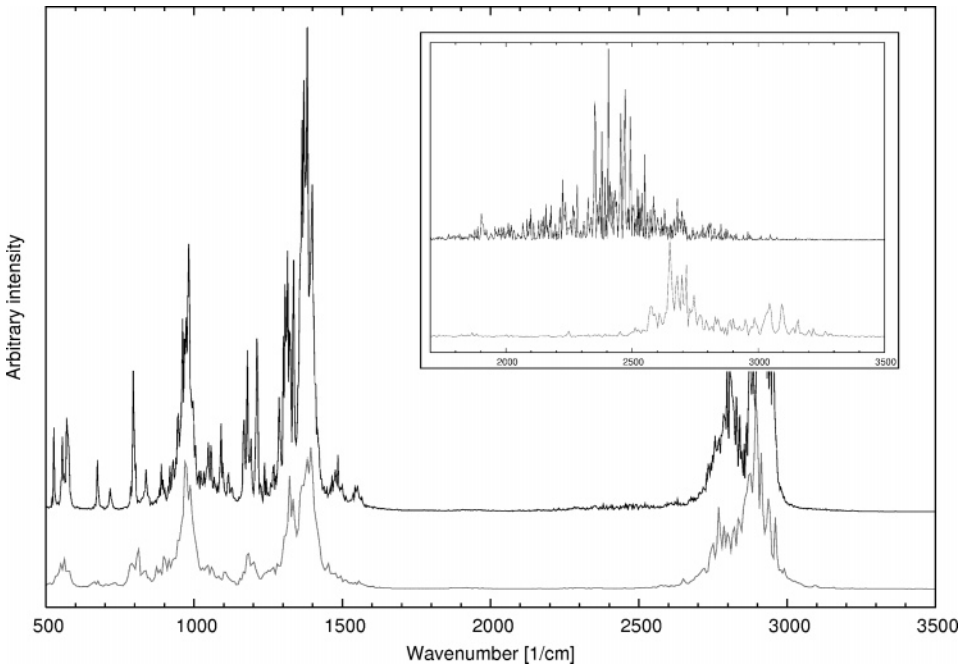

Figure 9. Comparison of the atomic velocity power spectra for the TMM molecule in the solid state (black) and in vacuo (gray). Inset: the O−H stretching region, contribution of the H2 hydrogen bridge proton.

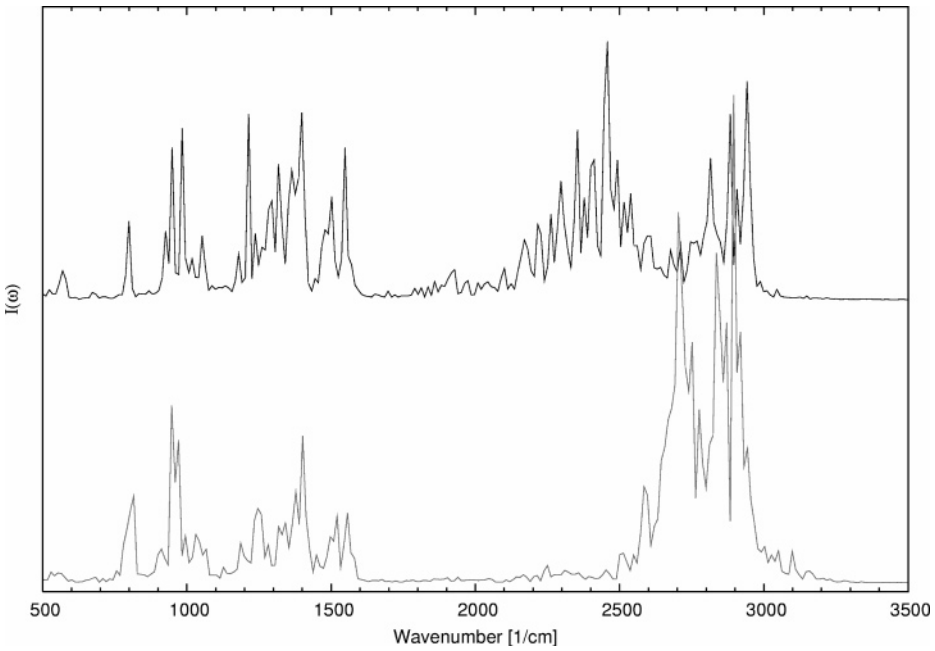

Figure 10. Comparison of predicted IR spectra for the TMM molecules in the solid state (top, black line) and in vacuo (bottom, gray line).

with an intensity increase characteristic of a hydrogen bond. The experimental spectral data of Filarowski et al.[60] were recorded in CCl_4 solution. The solvent molecules have vanishing dipole and quadrupole moments. Therefore, a comparison with gas-phase MD calculations is possible with caution. The reason for our reference to the liquid results in the context of our gas-phase MD is the need for establishing the qualitative accuracy of our computational model. The experimental OH stretching is in the range of 2200−3400 cm^{-1}, which is in very good agreement with our MD-based simulation, considering the applied approximations. The similarity of the gas-phase and CCl_4 environments has been investigated experimentally,[80] and it was found that the OH stretching mode red shift imposed by the solvent is usually 100−150 cm^{-1}, which corresponds to a ca. 1 kcal/mol increase in the hydrogen-bond energy.

Influence of the aromatic ring substituents on the hydrogen-bond strength is also reflected in the position and intensity of the OH stretching band. An experimental IR study[81] has shown that the intramolecular bond results in a smaller absorption coefficient when compared to a corresponding intermolecular case. Indeed, the intramolecular bond is energetically weaker, but favored by entropy. Methyl substituents in the ring are almost inert with respect to the OH stretching position—reported values for various CH_3 substitutions range from 2900 to 2906 cm^{-1}, with the important exception of the TMM molecule.[81] As mentioned above, the methyl groups in the 3 and 6 positions influence directly

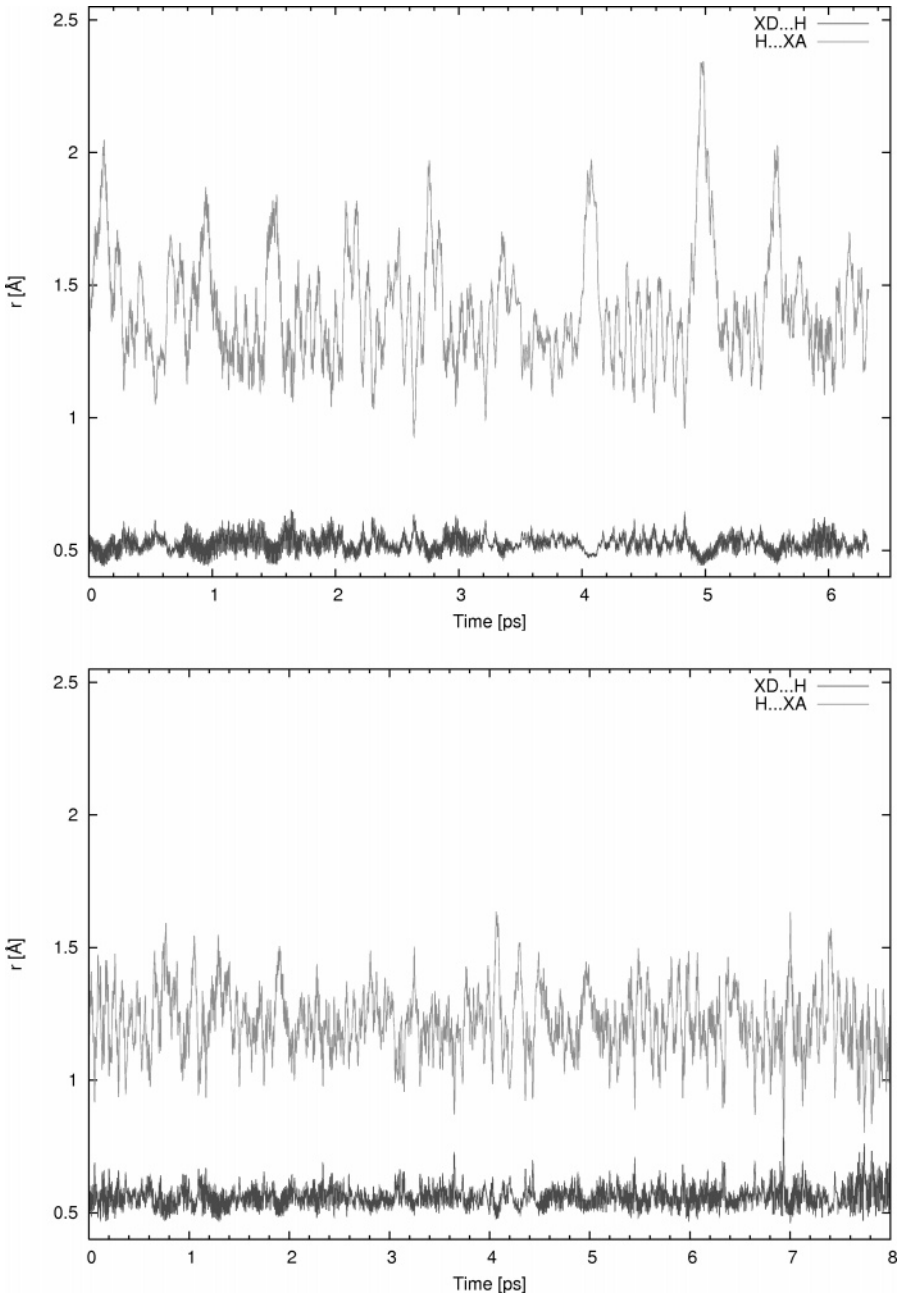

Figure 11. Time evolution of the distances between the bridge hydrogen atom (H) and Wannier function centers at the donor (XD) or acceptor (XA). Upper chart: gas-phase results. Lower chart: solid-state values.

the hydrogen bridge by sterical squeezing, which results in shortened and strengthened O−H···N interaction.[60] More active substituents (−Cl and $-NO_2$) can red-shift the OH band position down to 2478 cm^{-1} (for the 3,4,5,6-tetrachloro derivative). There is no clear experimental correlation between this red shift and position or type of the introduced group, apart from the fact that the larger the number of the substituents, the larger is the shift. A comparative computational study of substituent effects on the spectroscopic properties of Mannich base type compounds will be presented elsewhere as an extension of the current work.

The simulated spectrum indicates that the proton potential is indeed fluctuating, but within rather narrow limits. The spectroscopic evidence, both experimental and theoretical, suggests the proton residing at the donor oxygen atom in the hydrogen bridge of the studied TMM molecule in vacuo. The time evolution of the hydrogen-bridge distance parameters in the gas-phase simulation (Figure 6) supports this observation. The OH distance is well-defined and does not exhibit large fluctuations. Meanwhile, the O···N and, therefore, also the H···N distances seem to be very flexible. Their small modulating effect on the OH bond is, however, evident, especially at 3.3, 4.2, and 4.9 ps simulation times. At these points, the O···N separation is especially large, which immediately results in a decreased O−H bond length. This coupling of O···N and OH motions leads to neither proton transfer nor even proton sharing events. The average O···N distance calculated from the recorded CPMD trajectory is 2.684 Å (see Table 2 for comparison with the experimental data).

The solid-state CPMD simulation, based on the experimental X-ray structure of TMM,[60] is the next part of our study. The experimental solid-state IR spectrum, described in the Spectroscopic Data Analysis section, suggests that the

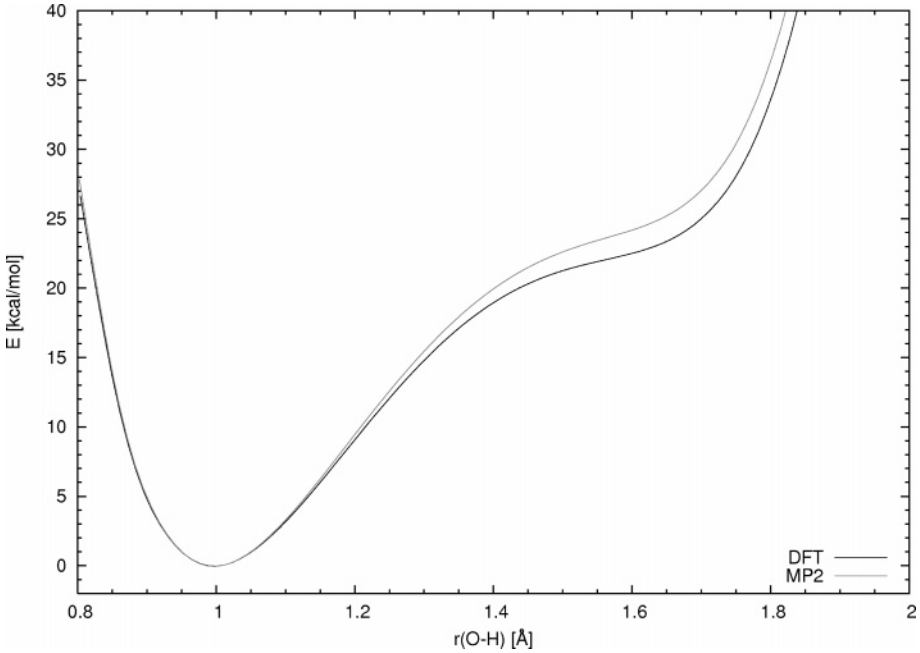

Figure 12. Potential energy function of a proton in the hydrogen bond of the TMM molecule, obtained from DFT and MP2 calculations with the cc-pVDZ basis set.

bridge proton is more delocalized in the polar environment of the crystal than in the gas phase or CCl_4 solution. During the simulation, all four TMM molecules of the unit cell were studied, giving essentially identical results. One of the molecules was selected for a detailed description (see Figure 2). The atomic velocity power spectrum is presented in Figure 7. The bridge proton contribution is located in the 800−1600 cm^{-1} and 1900−3000 cm^{-1} regions. The maximal motion intensity in the OH stretching region is reached between 2400 and 2500 cm^{-1}. The predicted IR spectrum derived from the dipole moment trajectory is presented in Figure 3, with the experimental solid-state spectrum shown in the inset. It confirms the atomic velocity power spectrum analysis, and the intensities of the OH stretching are very large, with a peak at 2450 cm^{-1}. The delocalization of the proton position is therefore significantly more vulnerable to environmental influence. The calculated spectroscopic CPMD results (see Table 1) are in good agreement with the experimental data. We can conclude that the CPMD simulation proved to be effective in the qualitative reproduction of the vibrational properties of the TMM crystal.

The hydrogen-bridge parameters recorded for the chosen molecule of the simulated TMM unit cell are presented in Figure 8. Several differences with respect to the gas-phase results (Figure 6) are worth discussing. Proton-transfer phenomena do not occur, but the proton is more labile, and at several points of the CPMD run, the proton−donor and proton−acceptor distances are almost equal. The second interesting fact is that the O···N fluctuations are smaller than in the gas phase, while the H···N distance is much more flexible. The calculated average O···N distance after ca. 12 ps of the CPMD run is 2.600 Å, which is only slightly smaller than the experimental X-ray value of 2.628(3) Å.[60] The corresponding gas-phase value (2.684 Å) reflects the relatively weaker hydrogen bond (see the data collected in Table 2).

In order to demonstrate clearly the influence of the environment on the bridge proton dynamics, the Fourier transforms of the atomic velocity and dipole moment autocorrelation functions are presented in Figures 9 and 10, respectively. Figure 9 shows that the modes other than those connected with the hydrogen bridge are virtually unaffected by the phase change, while the OH stretching region (shown in the inset) is significantly red-shifted in the solid state. This is also true for the spectrum derived from the dipole moment trajectory (Figure 10), where the broadening of the OH region is even more pronounced. Additionally, the hydrogen-bond presence is the dominant, most intensive feature of the solid-state spectrum.

The last step of the CPMD data analysis is the discussion of the hydrogen-bridge electronic structure. During the CPMD run, optimally localized Wannier functions[65,66] were calculated. The localization procedure corresponds to the Boys localization scheme, if the Γ-point approximation is used. The use of Wannier functions is an effective route to probe the electronic structure within the framework of a delocalized, periodic, plane-wave basis set.[82] The positions of the Wannier function centers were used to show the hydrogen-bridge bonding pattern. Figure 11 presents the time evolution of two such parameters: XD−H and H−XA distance, where XD and XA are Wannier centers of the donor−proton (oxygen) and proton−acceptor (nitrogen) bonds, respectively. While XD describes the O−H bond, XA is best described as the "center" of the nitrogen lone pair. The data shown in Figure 11 correspond well to the general picture drawn above based on the interatomic distances. In the gas phase, the XD−H length fluctuates within a very small range compared with the H−XA separation. However, the same modulating effect as that for O−H and H···N distances is evident. The electronic structure of the TMM hydrogen bridge in the gas phase is that of a donor-owned proton. This is less apparent in the case of the solid state,

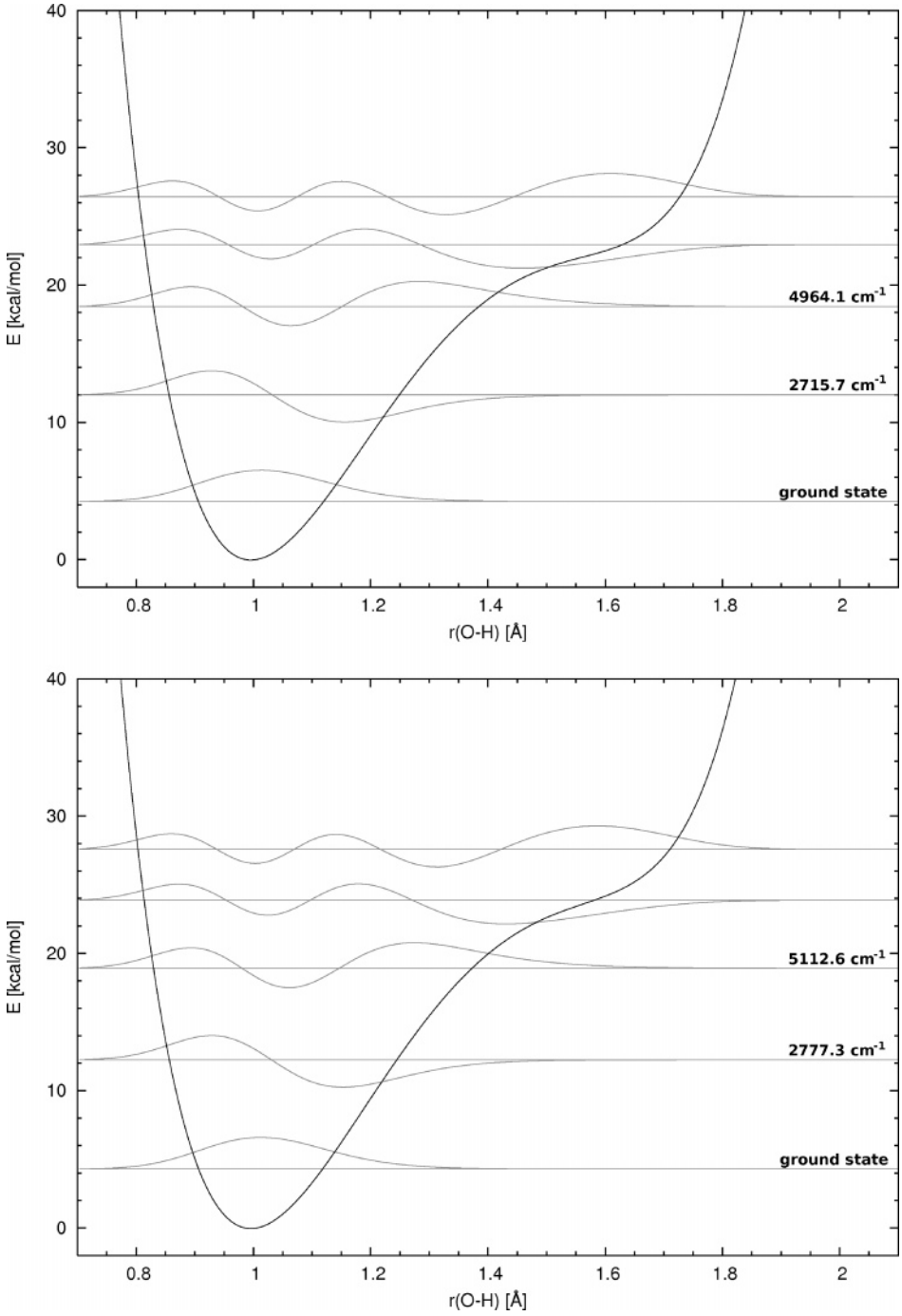

Figure 13. Anharmonic vibrational energy levels and wavefunctions resulting from solving the nuclear Schroedinger equation for the proton motion in the hydrogen bridge of the TMM molecule. Potential energy function calculated at the B3LYP/cc-pVDZ (top) and MP2/cc-pVDZ (bottom) levels.

where not only the XD−H fluctuations are larger, but the H−XA separation is more confined. Several cases of almost equal XD−H and H−XA parameters are directly related to the corresponding events recorded in the bond length time series (Figure 8). The results of this part of the study suggest that even the delocalized plane-wave basis set can be efficiently used in an electronic structure study of structurally flexible hydrogen bonds.

Results for the Static Models Based on DFT and MP2. Another approach applied to reproduce the potential energy surface (PES) of the OH stretching in the TMM molecule is a direct calculation of the energy versus the specified generalized coordinate (OH distance along the circular O··· ·N arc, as described in the Experimental and Computational Procedures section) using the optimized structure as the reference point. DFT and MP2 electronic structure methods were used to sample the PES and construct a one-dimensional model of it. The results obtained in this way are presented in Figure 12 and Table 1. We have declared previously that these results are not functionally equivalent to the CPMD spectra—the one-dimensional potential functions will not describe the modulating effect of the O···N stretching. The role of static models is therefore the estimation of the importance of the anharmonicity and quantum effects on the

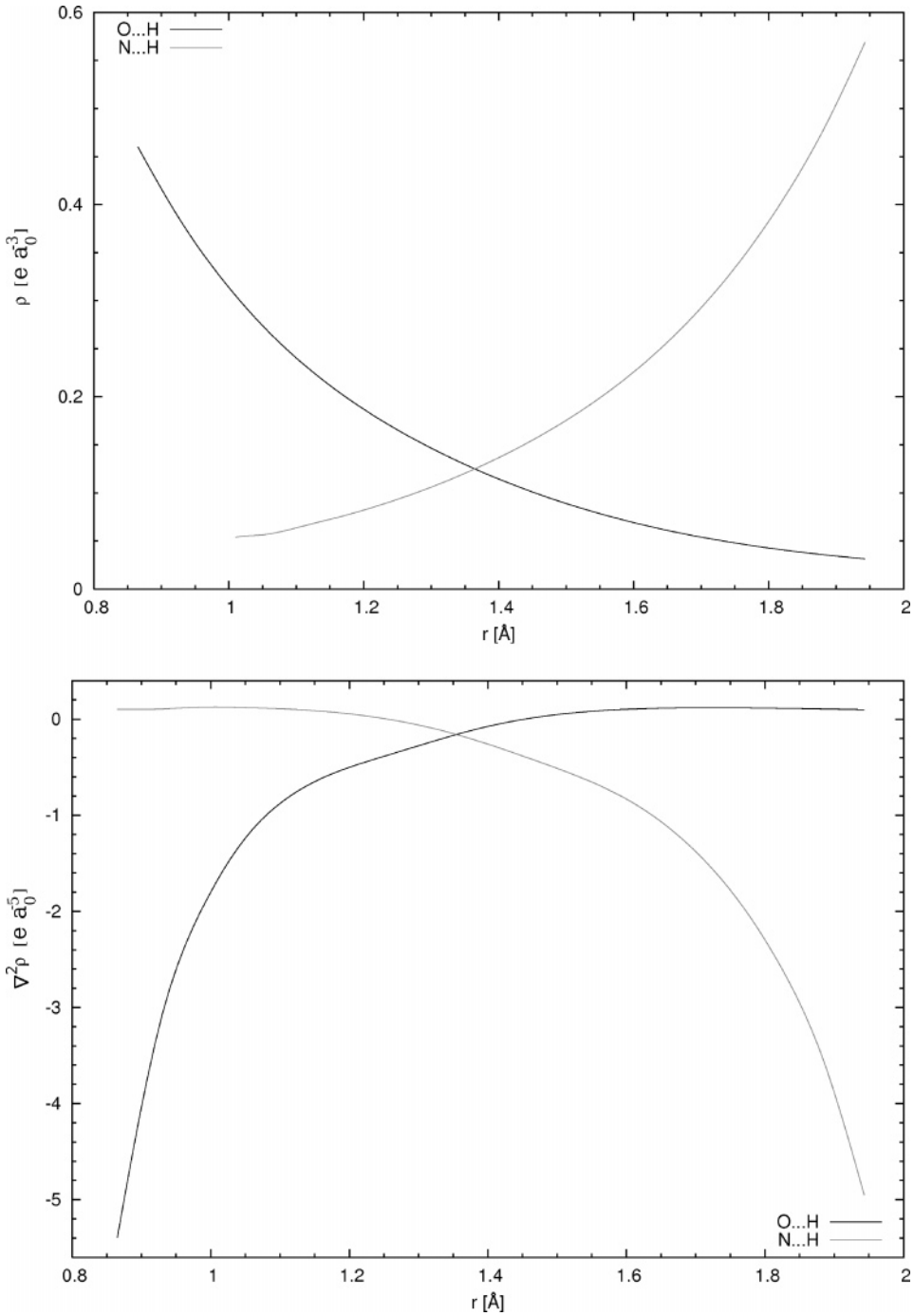

Figure 14. Electron density (top) and its Laplacian (bottom) calculated at each point of the circular path of the proton motion for the interaction between the indicated atoms.

proton motion. The calculated DFT-based PES has only one minimum on the donor (oxygen) side. The absence of the second minimum above 1.6 Å suggests that the proton transfer form is not present, in agreement with experimental observations. The potential energy function has only an inflection point on the acceptor side; moreover, this point is only slightly lower in energy on the DFT PES than on the MP2 PES. This proves that both the B3LYP DFT functional and the MP2 method provide similar descriptions of the proton potential. Even if the two PES functions look similar, they have different curvatures which will be reflected in the calculated vibrational frequencies. The anharmonicity of the OH stretching PES prompted us to apply the quantization of this particular mode by considering the quantum nature of the proton. The resulting vibrational energy levels and wavefunctions for both the DFT and MP2 data are presented in Figure 13. The calculated $0 \rightarrow 1$ frequencies for DFT (2715.7 cm^{-1}) and MP2 (2777.3 cm^{-1}) correspond well to the regions of the most intense motions in the gas-phase atomic velocity power spectra (see Table 1 and Figure 4) and in the experimental IR spectrum in CCl_4 solution reported by Filarowski et al.[60]

As the last point of our study, an AIM analysis of the electron density was performed for all proton positions on the circular path described above. The electron density and its Laplacian were calculated for each resulting structure at

two stationary points corresponding to the O−H and H···N interaction and are presented in Figure 14. These points cannot be called bond critical points in the spirit of the AIM theory because the analyzed TMM forms with displaced protons are not equilibrium structures. The electron density at the OH interaction point gradually diminishes with growing OH distance, while the NH interaction becomes stronger. The graph of the electron density Laplacian presents more descriptive information and enables us to distinguish three different regions of the proton PES. The first region, up to a 1.2 Å OH distance, is attributed to the elongated OH bond. The next, from 1.2 to 1.6 Å, describes the shared proton, while the last region (OH distance above 1.6 Å) suggests complete proton transfer to the acceptor site. The proton is shared exactly by the two heavy (donor and acceptor) atoms at a 1.35 Å OH distance. None of the two investigated electronic structure parameters display any abrupt change in the character of the donor−proton and proton−acceptor interactions, and there is a smooth transition from values prescribed by the Popelier criteria[75] to the much stronger ones describing the respective covalent bonds. However, it must be remembered that the analysis presented here was performed for nonequilibrium structures, for which AIM-based critieria might not necessarily apply.

IV. CONCLUSIONS

In this paper, we reported a detailed study of the vibrational properties of TMM, a Mannich base type compound. The computational part of the study was performed in the gas phase and the solid state. The obtained results explain the experimentally observed differences between TMM vibrational spectra recorded in various environments. The internal dynamics of the hydrogen bridge in the TMM compound were found to be strongly dependent on environmental influence, even if proton transfer was not induced throughout our simulation. Besides first-principle molecular dynamics, static DFT and MP2 models supported our discussion, indicating the level of anharmonicity of the OH stretching mode. Finally, topological analysis of the electron density was performed to provide insight into the phenomenon of proton sharing. Our computational results (especially full simulation of the IR spectrum) were compared with available experimental data, and good agreement between them was found.

ACKNOWLEDGMENT

The authors would like to thank Dr. Harald Forbert for the program for dipole moment transformations. In addition, the authors would like to thank Dr. Axel Kohlmeyer for creating a repository of CPMD tutorials and hints. Finally, the authors gratefully acknowledge the Wrocław Center for Networking and Supercomputing (WCSS), the Academic Computer Center CYFRONET-KRAKÓW (Grants KBN/SGI/UWrocl/029/1998 KBN/SGI/UWrocl/078/2001), and the Poznań Supercomputing Center for providing computer time and facilities.

REFERENCES AND NOTES

(1) Freddolino, P. L.; Arkhipov, A. S.; Larson, S. B.; McPherson, A.; Schulten, K. Molecular Dynamics Simulations of the Complete Satellite Tobacco Mosaic Virus. *Structure* **2006**, *14*, 437−449.
(2) Warshel, A. *Computer Modeling of Chemical Reactions in Enzymes and Solutions*; John Wiley and Sons, Inc.: New York, 1991; p 109.
(3) Bala, P.; Grochowski, P.; Lesyng, B.; McCammon, J. A. Quantum-Classical Molecular Dynamics of Proton Transfer in Phospholipase A_2. In *Quantum Mechanical Simulation Methods For Studying Biological* Systems, 1st ed.; Bicout, D., Field, M., Eds.; Springer-Verlag: Berlin, Germany, 1996; pp 119−156.
(4) Schäfer, H.; Mark, A. E.; van Gunstern, W. F. Absolute Entropies from Molecular Dynamics Simulation Trajectories. *J. Chem. Phys.* **2000**, *113*, 7809−7817.
(5) White, R. P.; Meirovitch, H. A Simulation Method for Calculating the Absolute Entropy and Free Energy of Fluids: Application to Liquid Argon and Water. *Proc. Natl. Acad. Sci. U.S.A.* **2004**, *101*, 9235−9240.
(6) Mu, Y.; Stock, G. Conformational Dynamics of Trialanine in Water: A Molecular Dynamics Study. *J. Phys. Chem. B* **2002**, *106*, 5294−5301.
(7) Kubinyi, H. QSAR and 3D QSAR in Drug Design. Part 1: Methodology. *Drug Discovery Today* **1997**, *2*, 457−467.
(8) Kubinyi, H. *QSAR: Hansch Analysis and Related Approaches*, 1st ed.; VCH: Weinheim, Germany, 1993; pp 57−68.
(9) Gupta, S. P. *QSAR and Molecular Modeling*, 1st ed.; Springer-Verlag: London, U. K., 2006.
(10) Devillers, J. No-Free-Lunch Molecular Descriptors in QSAR and QSPR. In *Topological Indices and Related Descriptors in QSAR and QSPR*, 1st ed.; Devillers, J., Balaban, A. T., Eds.; CRC Press: Boca Raton, FL, 2000; pp 1−20.
(11) Benigni, R. SARs and QSARs of Mutagens and Carcinogens: Understanding Action Mechanisms and Improving Risk Assessment. In *Quantitative Structure−Activity Relationship Models of Mutagens and Carcinogens*; Benigni, R., Ed.; CRC Press: Boca Raton, FL, 2003; pp 259−282.
(12) Goodsell, D. S.; Morris, G. M.; Olson, A. J. Automated Docking of Flexible Ligands: Applications of AutoDock. *J. Mol. Recognit.* **1996**, *9*, 1−5.
(13) Rao, M. S.; Olson, A. J. Modelling of Factor Xa-Inhibitor Complexes: A Computational Flexible Docking Approach. *Proteins* **1999**, *34*, 173−183.
(14) Walters, W. P.; Stahl, M. T.; Murcko, M. A. Virtual Screening−An Overview. *Drug Discovery Today* **1998**, *3*, 160−178.
(15) Tonmunphean, S.; Kokpol, S.; Parasuk, V.; Wolschann, P.; Winger, R. H.; Liedl, K. R.; Rode, B. M. Comparative Molecular Field Analysis of Artemisinin Derivatives: Ab Initio versus Semiempirical Optimized Structures. *J. Comput.-Aided Mol. Des.* **1998**, *12*, 397−409.
(16) Buolamwini, J. K.; Assefa, H. CoMFA and CoMSIA 3D QSAR and Docking Studies on Conformationally-Restrained Cinnamoyl HIV-1 Integrase Inhibitors: Exploration of a Binding Mode at the Active Site. *J. Med. Chem.* **2002**, *45*, 841−852.
(17) Vidossich, P.; Cacsella, M.; Carloni, P. Dynamics and Energetics of Water Permeation through the Aquaporin Channel. *Proteins: Struct., Funct., Bioinf.* **2004**, *56*, 844−845.
(18) Piana, S.; Bucher, D.; Carloni, P.; Rothlisberger, U. Reaction Mechanism of HIV-1 Protease by Hybrid Car−Parrinello/Classical MD Simulations. *J. Phys. Chem. B* **2004**, *108*, 11139−11150.
(19) Gao, M.; Sotomayor, M.; Villa, E.; Lee, E.; Schulten, K. Molecular Mechanisms of Cellular Mechanics. *Phys. Chem. Chem. Phys.* **2006**, *8*, 3692−3702.
(20) Maiti, A.; Sierka, M.; Andzelm, J.; Golab, J.; Sauer, J. Combined Quantum Mechanics: Interatomic Potential Function Investigation of Rac-Meso Configurational Stability and Rotational Transition in Zirconocene-Based Ziegler-Natta Catalysts. *J. Phys. Chem. A* **2000**, *104*, 10932−10938.
(21) Deglmann, P.; Ahlrichs, R.; Tsereteli, K. Theoretical Studies of Ligand-Free Cadmium Selenide and Related Semiconductor Clusters. *J. Chem. Phys.* **2002**, *116*, 1585−1587.
(22) Khriachtchev, L.; Novikov, S.; Räsänen, M. Laser-Controlled Stress of Si Nanocrystals in a Free-Standing Si/SiO_2 Superlattice. *Appl. Phys. Lett.* **2005**, *88*, 013102.
(23) Häkkinen, H.; Barnett, R. N.; Scherbakov, A. G.; Landman, U. Nanowire Gold Chains: Formation Mechanisms and Conductance. *J. Phys. Chem. B* **2000**, *104*, 9063−9066.
(24) Hod, O.; Baer, R.; Rabani, E. Feasible Nanometric Magnetoresistance Devices. *J. Phys. Chem. B* **2004**, *108*, 14807−14810.
(25) Hod, O.; Baer, R.; Rabani, E. A Parallel Electromagnetic Molecular Logic Gate. *J. Am. Chem. Soc.* **2005**, *127*, 1648−1649.
(26) Müller, A.; Ratajczak, H.; Junge, W.; Dieman, E.; Zundel, G. *Electron and Proton Transfer in Chemistry and Biology*; Elsevier: Amsterdam, The Netherlands, 1992.
(27) Zundel, G. Proton Polarizability of Hydrogen Bonds: Infrared Methods, Relevance to Electrochemical and Biological Systems. *Methods Enzymol.* **1986**, *127*, 439−455.

(28) Car, R.; Parrinello, M. Unified Approach for Molecular Dynamics and Density-Functional Theory. *Phys. Rev. Lett.* **1985**, *55*, 2471−2474.

(29) Doerksen, R. J.; Chen, B.; Klein, M. L. Intramolecular Hydrogen Bonds: Ab Initio Car−Parrinello Simulations of Arylamide Torsions. *Chem. Phys. Lett.* **2003**, *380*, 150−157.

(30) Romero, A. H.; Silvestrelli, P. L.; Parrinello, M. Compton Scattering and the Character of the Hydrogen Bond in Ice I_h. *J. Chem. Phys.* **2001**, *115*, 115−123.

(31) Rovira, C.; Novoa, J. J.; Ballone, P. Hydrogen Bonding and Collective Proton Modes in Clusters and Periodic Layers of Squaric Acid: A Density Functional Theory. *J. Chem. Phys.* **2001**, *115*, 6406−6417.

(32) Leung, K.; Rempe, S. B. Ab Initio Molecular Dynamics Study of Glycine Intramolecular Transfer in Water. *J. Chem. Phys.* **2005**, *122*, 184506.

(33) Boero, M.; Terakura, K.; Ikeshoji, T.; Liew, Ch.; Parrinello, M. Hydrogen Bonding and Dipole Moment of Water at Supercritical Conditions: A First-Principle Molecular Dynamics Study. *Phys. Rev. Lett.* **2000**, *85*, 3245−3248.

(34) Marx, D.; Hutter, J. Ab Initio Molecular Dynamics: Theory and Implementation. In *Modern Methods and Algorithms of Quantum Chemistry*; Grotendorst, J., Ed.; NIC: Jülich, Germany, 2000; Vol. 3, pp 329−477.

(35) Silvestrelli, P. L.; Bernasconi, M.; Parrinello, M. Ab Initio Liquid Spectrum of Liquid Water. *Chem. Phys. Lett.* **1997**, *277*, 478−482.

(36) Doltsinis, N. L.; Marx, D. First Principles Molecular Dynamics Involving Excited States and Nonadiabatic Transitions. *J. Theor. Comput. Chem.* **2002**, *1*, 319−349.

(37) Langer, H.; Doltsinis, N. L. Excited State Tautomerism of the DNA Base Guanine: A Restricted Open-Shell Kohn−Sham Study. *J. Chem. Phys.* **2003**, *118*, 5400−5407.

(38) Tuckerman, M. E.; Marx, D.; Klein, M. L.; Parrinello, M. On the Quantum Nature of the Shared Proton in Hydrogen Bonds. *Science* **1997**, *275*, 817−820.

(39) Laio, A.; VandeVondele, J.; Röthlisberger, U. A Hamiltonian Electrostatic Coupling Scheme for Hybrid Car−Parrinello Molecular Dynamics Simulations. *J. Chem. Phys.* **2002**, *116*, 6941−6948.

(40) Fatmi, M. Q.; Hofer, T. S.; Randolf, B. R.; Rode, B. M. An Extended ab Initio QM/MM MD Approach to Structure and Dynamics of Zn-(II) in Aqueous Solution. *J. Chem. Phys.* **2005**, *123*, 054514.

(41) Das, D.; Eurenius, K. P.; Billings, E. M.; Sherwood, P.; Chatfield, D. C.; Hodošček, M.; Brooks, B. R. Optimization of Quantum Mechanical Molecular Mechanical Partitioning Schemes: Gaussian Delocalization of Molecular Mechanical Charges and the Double Link Atom Method. *J. Chem. Phys.* **2002**, *117*, 10534−10547.

(42) Fedorowicz, A.; Mavri, J.; Bala, P.; Koll, A. Molecular Dynamics Study of the Tautomeric Equilibrium in the Mannich Base. **1998**, *289*, 457−462.

(43) Merzel, F.; Hodošček, M.; Janežič, D.; Sanson, A. New Force Field for Calcium Binding Sites in Annexin-Membrane Complexes. *J. Comput. Chem.* **2006**, *27*, 446−452.

(44) Sulpizi, M.; Rothlisberger, U.; Carloni, P. Molecular Dynamics Studies of Caspase-3. *Biophys. J.* **2003**, *84*, 2207−2216.

(45) Hohenberg, P.; Kohn, W. Inhomogeneous Electron Gas. *Phys. Rev.* **1964**, *136*, B864−B871.

(46) Møller, C.; Plesset, M. S. Note on an Approximation Treatment for Many-Electron Systems. *Phys. Rev.* **1934**, *46*, 618−622.

(47) Vashishtha, S. C.; Zello, G. A.; Nienaber, K. H.; Balzarini, J.; De Clercq, E.; Stables, J. P.; Dimmock, J. R. Cytotoxic and Anticonvulsant Aryloxyaryl Mannich Bases and Related Compounds. *Eur. J. Med. Chem.* **2004**, *39*, 27−35.

(48) Pandeya, S. N.; Sriram, D.; Nath, G.; De Clercq, E. Synthesis, Antibacterial, Antifungal and Anti-HIV Evaluation of Norfloxacin Mannich Bases. *Sci. Pharm.* **1999**, *67*, 103−111.

(49) Varma, R. S.; Nobles, W. L. Antiviral, Antibacterial, and Antifungal Activities of Isatin N-Mannich Bases. *J. Pharm. Sci.* **1975**, *64*, 881−882.

(50) Pandeya, S. N.; Sriram, D.; Nath, G.; De Clercq, E. Synthesis, Antibacterial, Antifungal and Anti-HIV Evaluation of Schiff and Mannich Bases of Isatin Derivatives with 3-Amino-2-methylmercapto quinazolin-4(3H)-one. *Pharm. Acta Helv.* **1999**, *74*, 11−17.

(51) Pandeya, S. N.; Sriram, D.; Nath, G.; De Clercq, E. Synthesis and Antimicrobial Activity of Schiff and Mannich Bases of Isatin and Its Derivatives with Pyrimidine. *Farmaco* **1999**, *54*, 624−628.

(52) Varma, R. S.; Nobles, W. L. Synthesis and Antiviral and Antibacterial Activity of Certain N-Dialkylaminomethylisatin Beta-Thiosemicarbazones. *J. Med. Chem.* **1967**, *10*, 972−974.

(53) Logan, J. C.; Fox, M. P.; Morgan, J. M.; Makohon, A. M.; Pfau, C. J. Arenavirus Inactivation on Contact with N-Substituted Isatin Beta-Thiosemicarbazones and Certain Cations. *J. Gen. Virol.* **1975**, *28*, 271−283.

(54) Imam, S. A.; Varma, R. S. Isatin-3-anils as Excystment and Cysticidal Agents against Schizopyrenus russelli. *Experienta* **1975**, *31*, 1287−1288.

(55) Holla, B. S.; Udupa, K. V. Synthesis of Novel 5-Mercapto-s-triazolo-[3,4-c]-as-triazino[5,6-b]indoles and Their Mannich Bases. *Heterocycles* **1991**, *32*, 1081−1088.

(56) Mitsch, A.; Wissner, P.; Sattler, I.; Schlitzer, M. Non-Thiol Farnesyltransferase Inhibitors: Structure−Activity Relationships of Aralkyl-subsituted Benzophenones. *Arch. Pharm. Med. Chem.* **2001**, *334*, 40−44.

(57) Sasse, A.; Ligneau, X.; Sadek, B.; Elz, S.; Pertz, H.; Ganelin, C. R.; Arrang, J. M.; Schwartz, J. C.; Schunack, W. Benzophenone Derivatives and Related Compounds as Potent Histamine H3-reCeptor Antagonists and Potential PET/SPECT Ligands. *Arch. Pharm. Med. Chem.* **2001**, *334*, 45−52.

(58) Tramontini, M.; Angiolini, L.; Ghednini, W. Mannich Bases in Polymer Chemistry. *Polymer* **1988**, *29*, 771−788.

(59) Koll, A.; Wolschann, P. Mannich Bases as Model Compounds for Intramolecular Hydrogen Bonding. I. Solid State Structures and Molecular Calculations. *Monatsh. Chem.* **1996**, *127*, 475−486.

(60) Filarowski, A.; Szemik-Hojniak, A.; Gowiak, T.; Koll, A. Anomalous Strengthening of the Intramolecular Hydrogen Bond by Steric Repulsion. *J. Mol. Struct.* **1997**, *404*, 67−74.

(61) *CPMD*; IBM Corp.: Armonk, NY, 1990−2004; MPI fuer Festkoerperforschung Stuttgart: Stuttgart, Germany, 1997−2001.

(62) Schlegel, H. B. Estimating the Hessian for Gradient-Type Geometry Optimizations. *Theor. Chim. Acta* **1984**, *66*, 333−340.

(63) Perdew, J. P.; Burke, K.; Ernzerhof, M. Generalized Gradient Approximation Made Simple. *Phys. Rev. Lett.* **1996**, *77*, 3865−3868.

(64) Troullier, N.; Martins, J. L. Efficient Pseudopotentials for Plane-Wave Calculations. *Phys. Rev. B: Condens. Matter Mater. Phys.* **1991**, *43*, 1993−2006.

(65) Marzari, N.; Vanderbilt, D. Maximally Localized Generalized Wannier Functions for Composite Energy Bands. *Phys. Rev. B: Condens. Matter Mater. Phys.* **1997**, *56*, 12847−12865.

(66) Silvestrelli, P. L. Maximally Localized Wannier Functions for Simulations with Supercells of General Symmetry. *Phys. Rev. B: Condens. Matter Mater. Phys.* **1999**, *59*, 9703−9706.

(67) Kendall, R. A.; Dunning, T. H., Jr.; Harrison, R. J. Electron Affinities of the First-Row Atoms Revisited. Systematic Basis Sets and Wave Functions. *J. Chem. Phys.* **1992**, *96*, 6796−6806.

(68) Woon, D. E.; Dunning, T. H., Jr. Gaussian Basis Sets for Use in Correlated Molecular Calculations. III. The Atoms Aluminum through Argon. *J. Chem. Phys.* **1993**, *98*, 1358−1371.

(69) Becke, A. D. Density-Functional Thermochemistry. III. The Role of Exact Exchange. *J. Chem. Phys.* **1993**, *98*, 5648−5652.

(70) Lee, C.; Yang, W.; Parr, R. G. Development of the Colle−Salvetti Correlation-Energy Formula into a Functional of the Electron Density. *Phys. Rev. B: Condens. Matter Mater. Phys.* **1988**, *37*, 785−789.

(71) Frisch, M. J.; Trucks, G. W.; Schlegel, H. B.; Scuseria, G. E.; Robb, M. A.; Cheeseman, J. R.; Montgomery, J. A., Jr.; Vreven, T.; Kudin, K. N.; Burant, J. C.; Millam, J. M.; Iyengar, S. S.; Tomasi, J.; Barone, V.; Mennucci, B.; Cossi, M.; Scalmani, G.; Rega, N.; Petersson, G. A.; Nakatsuji, H.; Hada, M.; Ehara, M.; Toyota, K.; Fukuda, R.; Hasegawa, J.; Ishida, M.; Nakajima, T.; Honda, Y.; Kitao, O.; Nakai, H.; Klene, M.; Li, X.; Knox, J. E.; Hratchian, H. P.; Cross, J. B.; Bakken, V.; Adamo, C.; Jaramillo, J.; Gomperts, R.; Stratmann, R. E.; Yazyev, O.; Austin, A. J.; Cammi, R.; Pomelli, C.; Ochterski, J. W.; Ayala, P. Y.; Morokuma, K.; Voth, G. A.; Salvador, P.; Dannenberg, J. J.; Zakrzewski, V. G.; Dapprich, S.; Daniels, A. D.; Strain, M. C.; Farkas, O.; Malick, D. K.; Rabuck, A. D.; Raghavachari, K.; Foresman, J. B.; Ortiz, J. V.; Cui, Q.; Baboul, A. G.; Clifford, S.; Cioslowski, J.; Stefanov, B. B.; Liu, G.; Liashenko, A.; Piskorz, P.; Komaromi, I.; Martin, R. L.; Fox, D. J.; Keith, T.; Al-Laham, M. A.; Peng, C. Y.; Nanayakkara, A.; Challacombe, M.; Gill, P. M. W.; Johnson, B.; Chen, W.; Wong, M. W.; Gonzalez, C.; Pople, J. A. *Gaussian 03*, Revision C.02; Gaussian, Inc., Wallingford CT, 2004.

(72) Panek, J.; Stare, J.; Hadži, D. From the Isolated Molecule to Oligomers and the Crystal: A Static Density Functional Theory and Car−Parrinello Molecular Dynamics Study of Geometry and Potential Function Modifications of the Short Intramolecular Hydrogen Bond in Picolinic Acid *N*-Oxide. *J. Phys. Chem. A* **2004**, *108*, 7417−7423.

(73) Stare, J.; Mavri, J. Numerical Solving of the Vibrational Time-Independent Schrödinger Equation in One and Two Dimensions Using the Variational Method. *Comput. Phys. Commun.* **2002**, *143*, 222−240.

(74) Bader, R. F. W. *Atoms in Molecules − A Quantum Theory*, 1st ed.; Oxford University Press: Oxford, U. K., 1990; pp 169−351.

(75) Koch, U.; Popelier, P. L. A. Characterization of C−H···O Hydrogen Bonds Based on the Charge Density *J. Phys. Chem.* **1995**, *99*, 9747−9754.

(76) Biegler-König, F. W.; Bader, R. F. W.; Tang, T.-H. Calculation of the Average Properties of Atoms in Molecules. II. *J. Comput. Chem.* **1982**, *3*, 317−328.
(77) Portmann, S.; Lüthi, H. P. MOLEKEL: An Interactive Molecular Graphics Tool. *Chimia* **2000**, *54*, 766−770.
(78) Macrae, C. F.; Edgington, P. R.; McCabe, P.; Pidcock, E.; Shields, G. P.; Taylor, E.; Towler, M.; van de Streek, J. Mercury: Visualization and Analysis of Crystal Structures. *J. Appl. Crystallogr.* **2006**, *39*, 453−457.
(79) Allen, M. P.; Tildesley, D. J. *Computer Simulation of Liquids*; Clarendon Press: Oxford, U. K., 1994; pp 58−64.
(80) Rutkowski, K.; Koll, A. Gas Phase IR Spectra of Systems with Intramolecular Hydrogen Bonds. *J. Mol. Struct.* **1994**, *322*, 195−203.
(81) Filarowski, A.; Koll, A. Integrated Intensity of ν_s(OH) Absorption Bands in Bent Hydrogen Bonds in *ortho*-Dialkylaminomethylphenols. *Vib. Spectrosc.* **1996**, *12*, 15−24.
(82) Silvestrelli, P. L.; Marzari, N.; Vanderbilt, D.; Parrinello, M. Maximally-Localized Wannier Functions for Disordered Systems: Application to Amorphous Silicon. *Solid State Commun.* **1998**, *107*, 7−11.

CI600490S